Evaluation of Simple Amides in the Selective Recovery of Gold from Secondary Sources by Solvent Extraction

Evaluation of simple amides in the selective recovery of gold from secondary sources by solvent extraction.

Euan D. Doidge,[a†] Luke M. M. Kinsman,[a] Yiran Ji,[a] Innis Carson,[a] Andrew J. Duffy,[a] Izabela A. Kordas,[a] Eddie Shao,[a] Peter A. Tasker,[a] Bryne T. Ngwenya,[b] Carole A. Morrison,[a] and Jason B. Love[a].*

[a] *EaStCHEM School of Chemistry, David Brewster Road, The King's Buildings, University of Edinburgh, Edinburgh EH9 3FJ, UK.*

[b] *School of Geosciences, James Hutton Road, The King's Buildings, University of Edinburgh, Edinburgh EH9 3FE, UK.*

Corresponding author: Jason.love@ed.ac.uk

Keywords: Electronic Waste, Recycling, Supramolecular, Computational, WEEE

ABSTRACT. The recycling of metals from end-of-life secondary sources such as electronic waste remains a significant environmental and technological challenge currently detrimental to the development of circular economies. The complex nature of electronic waste, containing a myriad of different elemental metals, means that sophisticated yet simple separation methods need to be developed in order to recycle these valuable and often critical metal resources. In this work simple

primary, secondary, and tertiary amides are appraised as reagents that selectively transport gold from aqueous to organic phases in a solvent extraction experiment. While the strength of extraction of gold from single metal solutions is ordered 3°>2°>1°, the 3° and 2° amides are ineffective at gold transport from mixed-metal solutions of concentrations representative of smartphones due to the formation of a third, dense phase. Increasing the polarity of the organic phase can negate third phase formation but at the expense of selectivity. The identities of the species that reside in the organic and third phases have been studied by a combination of slope analysis, mass spectrometry, NMR spectroscopy, and computational methods. These techniques show that protonation of the amide **L** occurs at the oxygen atom, resulting in the protonated dimer $H\mathbf{L}_2^+$ which acts as a receptor for $AuCl_4^-$ to form dynamic supramolecular aggregates in the organic phase. The characterization of a tin complex in the third phase by X-ray crystallography supports these conclusions and furthermore, suggests the preference for the chelation of the proton by two amide molecules instead of the transport of hydronium into the organic phase and its subsequent use as structural template.

INTRODUCTION

Gold is an important metal that is increasingly prevalent in modern technologies such as those found in electronics, catalysis and medicines due to its chemical and physical properties.[1-4] Much attention has been paid to the investigation of more efficient recovery and purification of gold due to the environmental and economic burden of recovering this scarce and sparsely distributed metal from primary sources, which requires energy- and emission-intense mining and separation processes.[5] There has been a recent drive to recycle gold and other metals from secondary sources such as Waste Electrical and Electronic Equipment (WEEE),[6] as this is a much more concentrated source of metals and could partly negate the high global-warming potential of gold

production.[7] [8] WEEE is recognized as the fastest-growing global waste stream (>5% annual growth) and comprises both critical and hazardous materials for which new separation and recycling technologies are required to provide impetus to global circular economy visions.[9-13]

Currently around 90% of the world's gold supply is derived from mining processes that exploit cyanidation. This process forms, through heap leaching, solutions of the water-soluble $Au(CN)_2^-$ complex, which is recovered from solution by precipitation, adsorption, and reduction.[14] The environmental and safety concerns over cyanidation has led to recent studies on alternative leaching and separation methods,[15] including the use of various combinations of oxidizing agents and organic solvents,[16-19] oxidative mechanochemistry,[20], electrochemical dissolution,[21] and Metal-Organic Framework (MOF) – polymer composites.[22-25]. These methods often result in the dissolution of gold through the formation of the halometalate AuX_4^-. Selective recovery of gold from aqueous solution has been achieved by co-precipitation of $AuBr_4^-$ with α-cyclodextrin as $\{[K(OH_2)_6][AuBr_4](\alpha\text{-cyclodextrin})_2\}_n$, forming chains of these components through supramolecular hydrogen-bonding and electrostatic interactions, creating an insoluble crystalline material that can be separated from the bulk material by simple filtration.[26] More recently, this system was applied to the recovery of gold from nanomaterials with life-cycle analysis indicating the application of this technology would reduce the environmental burden of gold nanoparticle synthesis.[27]

An alternative chemical separation method is solvent extraction which involves the selective transport of a single metal from an aqueous mixture of metals into a hydrophobic (organic) phase through coordination and/or supramolecular chemical recognition.[28] This scalable and economical method is used widely, producing high-purity metals in continuous flow with good materials balance.[29] Gold and other platinum group metals (PGMs) are often recovered and

refined in flowsheets that exploit separation by solvent extraction.[30] Here, the mixture of metals is first dissolved (leached) under oxidizing conditions in hydrochloric acid to form chloridometalates, MCl_n^{m-} which can be transported into a hydrophobic organic phase by protonatable reagents (**L**) to form organic-soluble, charge-neutral assemblies ($[MCl_n(LH)_m(\mathbf{L})_{y-m}]$) (Eq. 1). It is important that these reagents have both selectivity for one chloridometalate over the others present, and over other anions, particularly Cl^- as this is usually present in excess.[31]

$$MCl_n^{m-}{}_{(aq)} + y\,\mathbf{L}_{(org)} + m\,H^+_{(aq)} \rightleftharpoons [MCl_n(\mathbf{L}H)_m(\mathbf{L})_{y-m}]_{(org)} \qquad \text{Eq. 1}$$

We recently reported that the simple primary amide $\mathbf{L^1}$ (Figure 1) can strongly and selectively recover gold by solvent extraction from an aqueous mixture of metals representative of those found in WEEE.[32] The use of this reagent offers significant advantages over current commercial gold extractants through enhanced selectivity, efficiency, safety and overall mass-balance. It was seen that the primary amide $\mathbf{L^1}$ extracts gold as supramolecular assemblies of the gold(III) chloridometalate $AuCl_4^-$ and combinations of $\mathbf{L^1}$ and $H(\mathbf{L^1})_2^+$, e.g. $\{AuCl_4\}_4\{H(\mathbf{L^1})_2\}_4(\mathbf{L^1})_6$ as a result of enhanced hydrogen-bonding and Coulombic interactions in the hydrophobic medium.

The efficacy of $\mathbf{L^1}$ in the recovery of gold by solvent extraction is unusual as the general use of primary amides has not been widely reported and only for the extraction of f-block elements.[33] This lack of use is possibly attributed to an assumed lack of solubility in the hydrophobic medium or of the presence of multiple classical N-H bonds that can competitively extract chloride ions. In contrast, secondary and tertiary amides are more commonly used in platinum group metal (PGM) and other chloridometalate extraction as, due to the incorporation of more alkyl substituents at the amide nitrogen atoms, an increase in the lipophilicity of the extractant is seen.[28, 30, 34-36] The retention of the weakly basic amide functionality can provide diffuse, non-

classical C-H interactions that preferentially interact with the diffusely charged metalate anions over the chloride ions present in solution.[31]

Whilst expected to show enhanced selectivity for diffusely charged anions, multiply substituted secondary and tertiary amides can however exhibit poor phase-disengagement properties during the solvent extraction process, or be 'too strong' for gold recovery and not easily back-extracted to transfer the selected metalate into a fresh aqueous phase.[14, 28] To investigate these issues, and to determine the importance of the availability of hydrogen-bond donors and acceptors on these reagents for effective gold separation, we have prepared and evaluated here simple secondary (**L²**) and tertiary analogues (**L³**) of the primary amide **L¹** (Figure 1). While the removal of N-H bonds should favor non-classical hydrogen-bonding interactions with metalates and therefore aid extraction, the decrease in available hydrogen-bond donors may impact on the ability of **L²** and **L³** to form assemblies to the same extent as the primary amide **L¹**.

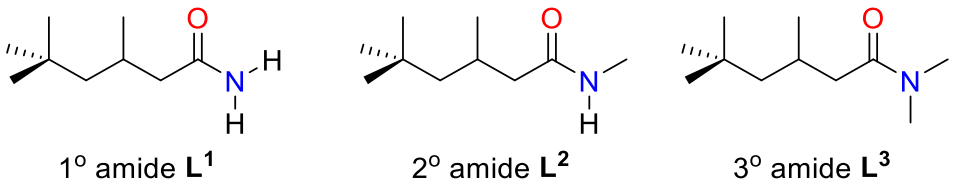

Figure 1. Structures of the series of simple primary (1°, **L¹**), secondary (2°, **L²**) and tertiary (3°, **L³**) amides.

RESULTS AND DISCUSSION

Characteristics of gold recovery by solvent extraction using L¹ – L³

The transport of gold from single-metal hydrochloric acid solutions of varying concentration into toluene solutions of the three amides **L¹-L³** was evaluated and shows a similar pattern for each

(Figure 2). As the concentration of HCl is increased, the amount of gold transported into the organic phase increases, reflecting an increasing propensity for the amides to become protonated and interact with the anionic metalates to form charge-neutral assemblies that are soluble in the organic phase. As the [HCl] increases further, the amount of gold in the organic phase decreases. This is a common feature of the transport of metalate anions in solvent extraction and is attributed to competing transport of chloride at much higher concentrations of HCl.

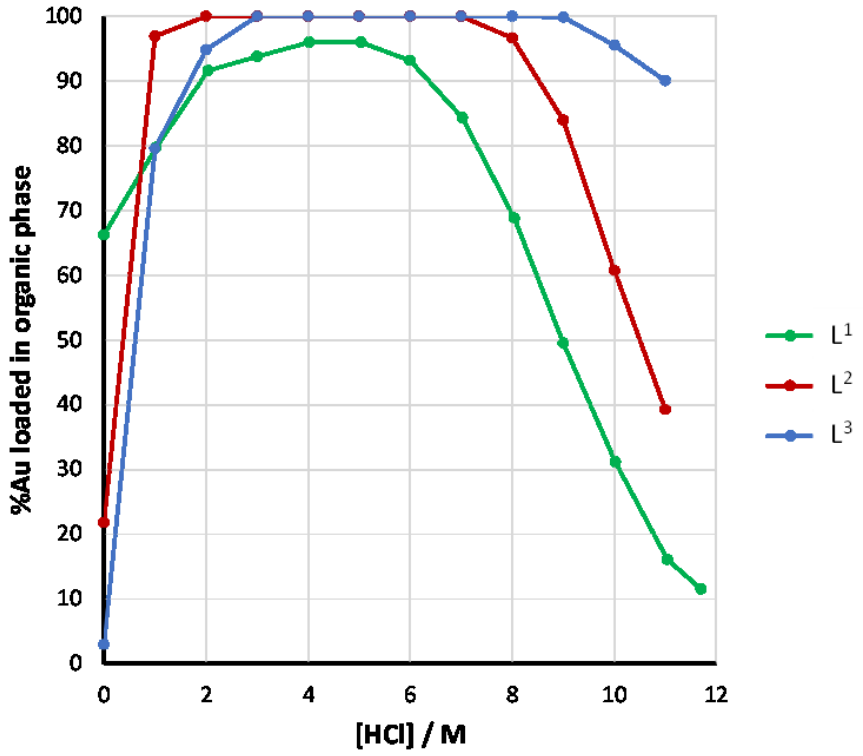

Figure 2. Transport of gold from aqueous solutions of varying [HCl] into a toluene solution of **L**^{1}, **L**^{2} or **L**^{3}. Conditions: $HAuCl_4$ (0.01 M) in 0-11 M HCl (2 mL) stirred with **L** (0.1 M) in toluene (2 mL); phases contacted for 1 h at RT.

The ability of the amides **L**^{2} and **L**^{3} to transport gold into the organic phase is greater than **L**^{1}, with the secondary amide reaching high levels of gold loading at lower [HCl] and the tertiary amide able to maintain high extraction at higher [HCl]. DFT geometry optimization calculations

were carried out in an attempt to rationalize these data. The formation of the receptor $H(\mathbf{L})_2^+$ for $AuCl_4^-$ transport is 30.9 kJ mol^{-1} more thermodynamically favorable for $\mathbf{L^3}$ than for $\mathbf{L^2}$, and a further 56.0 kJ mol^{-1} more favorable for $\mathbf{L^2}$ than $\mathbf{L^1}$. As such, this feature may contribute to the increased levels of gold transport by the more substituted amides at low [HCl]. Further calculations indicate that association of a chloride ion with a single protonated amide monomer $H(\mathbf{L})^+$ is significantly more favorable than association of a chloride ion to the equivalent protonated dimer $H(\mathbf{L})_2^+$ for all three amides, suggesting that the O-H---O hydrogen-bonding interactions within $H(\mathbf{L})_2^+$ are cleaved upon interaction with the chloride ion. The calculations indicate that this process is more thermodynamically favorable for less substituted amides, with the formation of [(H**L**)Cl] from $H(\mathbf{L})_2^+$ being 51.8 kJ mol^{-1} more favorable for $\mathbf{L^1}$ than for $\mathbf{L^2}$, and a further 15.9 kJ mol^{-1} more favorable for $\mathbf{L^2}$ compared to $\mathbf{L^3}$. The difference in favorability of these interactions between primary, secondary and tertiary amides can account for the increase in [HCl] at which gold extraction begins to decline.

Back-extraction (stripping) of gold-loaded organic phases using water

An important feature of the use of $\mathbf{L^1}$ in the recovery of gold by solvent extraction is the ability to back-transfer (strip) the organic-loaded gold metalate into a fresh aqueous solution to favor the production of the high-purity metal through reduction. Similar to the primary amide $\mathbf{L^1}$ reported previously, the gold-loaded secondary $\mathbf{L^2}$ and tertiary $\mathbf{L^3}$ amide toluene solutions are also back-extracted successfully using water, with 90% and 97% of gold transported into water on a single-contact with water, allowing the recycling of the ligand solutions to load gold multiple-times thereafter. Back-transfer of gold from organic phases containing tertiary monoamides has been reported to be successful on contact with water, albeit not quantitative (*ca.* 60-70%) and in some

cases thiourea-HCl solutions were required for complete stripping of the gold from the loaded organic phase to be achieved.[35-36]

Characterization of gold metalate assemblies in the organic phase

The L:M ratio in the assemblies formed in the organic phase can be inferred by analysis of the slope of a linear plot of log D (D = distribution coefficient = $[M]_{(org)}/[M]_{(aq)}$) vs. log [L]. However, the usefulness of this plot is reliant on a single species being extracted, and that any amide not involved in the extracted species is independent of the assembly.[30, 37] For the primary amide **L^1**, these L:M ratios were shown to vary from 2.5 to 3.0 and were dependent on the initial metal concentration.[32] Clusters of multiple amide and metalate units were identified in the organic phase, with these non-integer ratios indicating the presence of a mixture of species, or that surplus amide is interacting through hydrogen bonding to these supramolecular assemblies. Similarly, the slope analyses for the transport of Au(III), Fe(III) and Ga(III) with **L^2** and **L^3** also give a range of non-integer gradients (ranging from 2 to 3), suggesting that both of these amides extract the metals in a similar way to **L^1** (Figure S1).

The identity of the species formed in the organic phase was investigated by positive-ion ESI-MS. While it is clear that mass spectrometry will only probe the nature of the organic-phase speciation indirectly, it has been shown that in tandem with other techniques, e.g. computational and NMR studies, the information it offers can help define the organic-phase solution structures obtained. Gold-loaded toluene solutions of **L^2** and **L^3** diluted in CH_3CN were analyzed, and several gold-containing ions are seen. Previously for **L^1**, the +ESI-MS spectrum revealed the presence of ions of the general formula $[(AuCl_4)_n(H\mathbf{L^1}_2)(H\mathbf{L^1})_{n-1}]H^+$, up to n = 4, comprising a basic unit of $(AuCl_4)(H\mathbf{L^1}_2)H^+$, with higher m/z cations involving stepwise additions of $(AuCl_4)(H\mathbf{L^1})$.[32] No ions containing water or hydronium were detected, consistent with Karl-Fischer analyses of the

water-immiscible phases. The distinctive isotopic distribution pattern for each ion indicated that every gold atom retains four chlorides, consistent with the transport of $AuCl_4^-$ units through outer-sphere interactions (i.e. no chloride substitution occurs).

For gold-loaded solutions of **L²** and **L³**, the mass spectra are similar to those of **L¹** (Figures S4 and S5). The protonated dimer of the ligand is seen for each, with $(H\mathbf{L^2})_2^+$ at *m*/*z* 343 and $(H\mathbf{L^3})_2^+$ at *m*/*z* 371. While gold-containing ions of the form $[(AuCl_4)_n(H\mathbf{L}_2)(H\mathbf{L})_{n-1}]H^+$ are seen for **L²** and **L³**, clustered units containing more than one metalate are significantly less abundant than for **L¹**. This suggests that the secondary and tertiary amides are less able to form supramolecular aggregates with $AuCl_4^-$ than the primary amide and is consistent with the removal of N-H hydrogen-bond donors, limiting the hydrogen-bonding interactions between the metalate and the amide receptors.

The interactions between the amides **L¹**, **L²** and **L³** and metalates were studied further using classical molecular dynamics simulations. Three simulations were run for a total of 10.2 ns for each of **L¹**, **L²** and **L³**, with each simulation comprising ten amides of which four were protonated, four $AuCl_4^-$ anions and an explicit toluene solvent, contained within a periodic box of side length 60 Å (Figure 3); these ratios are derived from the slope analysis data and no water molecules were included (see later). In all simulations, bridging hydrogen-bonding interactions are seen between amides and multiple $AuCl_4^-$ anions, leading to the formation of supramolecular assemblies in which metalates are proximate to each other (Au…Au range 6.5 – 7.5 Å, Figure 4); these assemblies are stable for the duration of the simulation.

For **L¹** and **L²**, all four metalates are assimilated into a single assembly in all three simulations, which once formed remain intact during the MD simulation runs. This contrasts with **L³** in which a four metalate assembly is only seen in one out of three simulations, and even then only

transiently; clusters containing two or three metalate anions are more prevalent (see Figure 4 for an example cluster formed using **L**^{3}). For a more detailed analysis, the total count of amide N atoms found within a 4 Å distance from at least one chlorine atom over the course of the final 5 ns of MD production runs, expressed as a percentage of the maximum number of possible N…Cl interactions, were calculated; the interatomic distance of 4 Å is typical of hydrogen-bonding interactions that are responsible for clustering (Table 1, see SI for further detail).

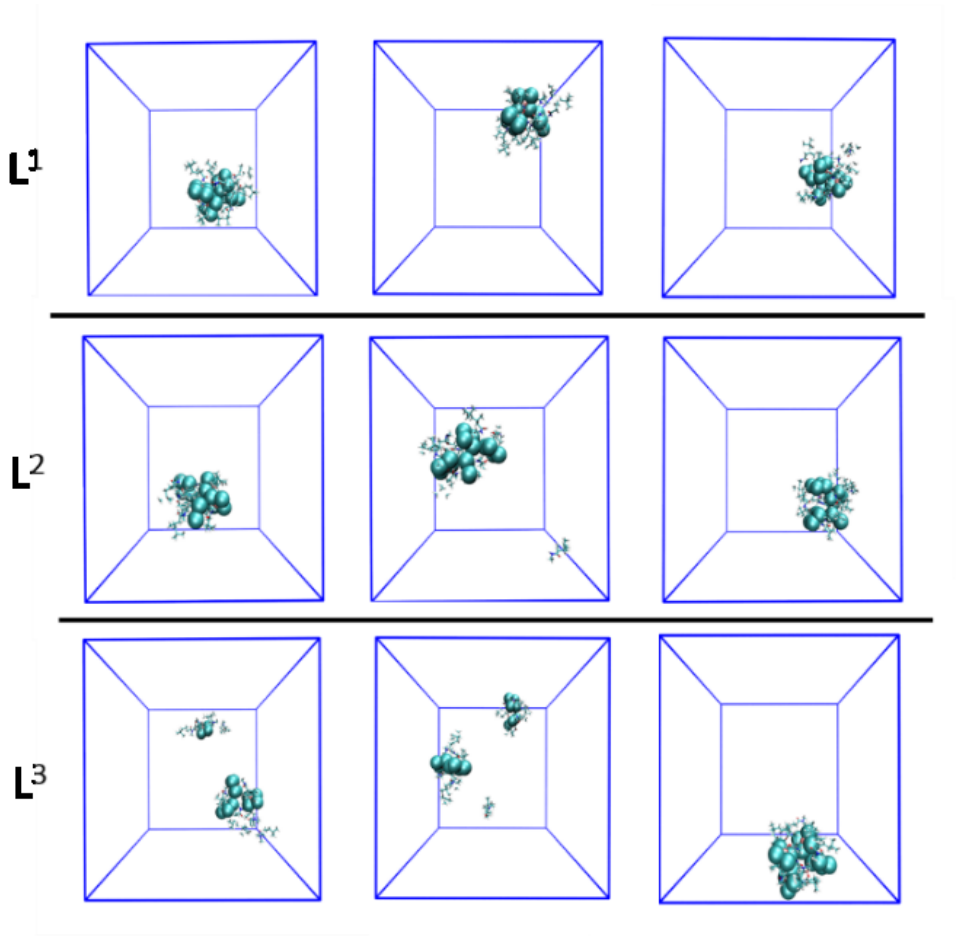

Figure 3. Representative geometries from classical molecular dynamics simulations involving four $AuCl_4^-$ units (shown in van der Waal representation), toluene solvent, and ten units of either **L**^{1} (upper), **L**^{2} (middle) or **L**^{3} (lower), of which four are protonated. For clarity, toluene molecules

are omitted. Formation of a single assembly incorporating all four $AuCl_4^-$ anions can be seen in all simulations except for two of those involving **L**^{3}.

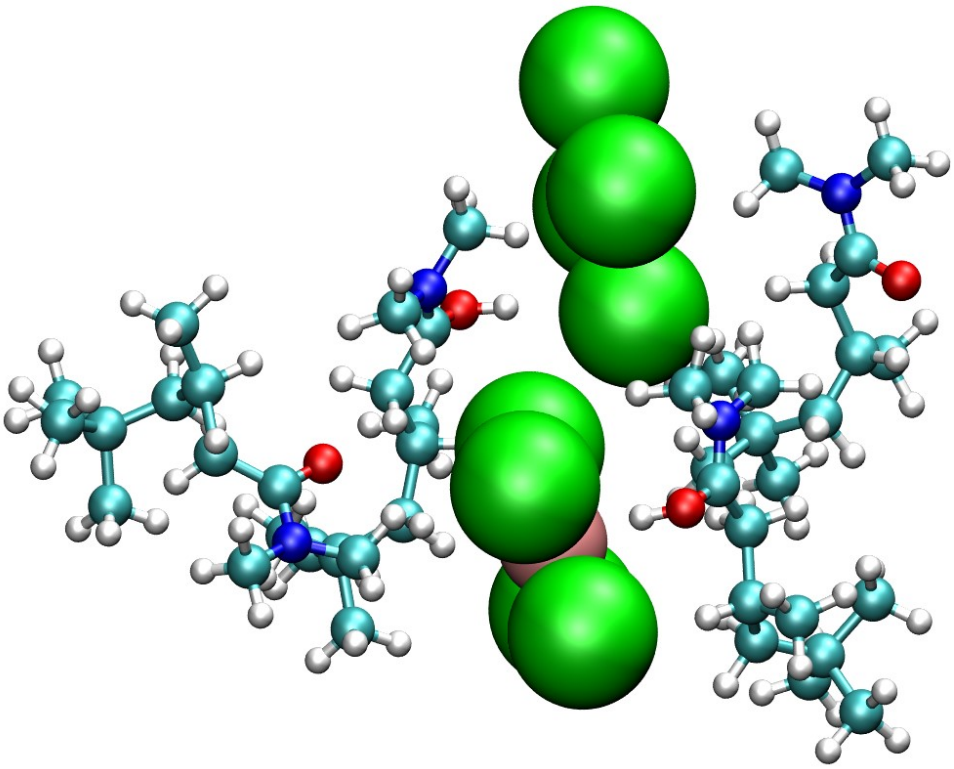

Figure 4. Example geometry of an assembly of $AuCl_4^-$, **L**^{3} and H(**L**^{3})$_2^+$ units obtained from a molecular dynamics simulation. See Figures S2 and S3 for typical clusters formed when using **L**^{1} or **L**^{2}.

Table 1. The percentage of amide nitrogen atoms located within a distance of 4 Å from at least one chlorine atom, expressed with respect to the theoretical maximum number, over the course of three molecular dynamics simulations.

	Simulation 1	Simulation 2	Simulation 3
L^1	66.0	66.2	62.5
L^2	47.9	43.3	43.0

L³	9.6	13.2	13.1

These analyses indicate that the amide groups in **L¹** and **L²** reside much closer to the metalate anions than the amide groups in **L³**. This can simply be attributed to N-H---Cl interactions, which are absent in the **L³**/$AuCl_4^-$ system. The presence of fewer hydrogen-bond donors in **L²** compared to **L¹** is also reflected in the data. Overall the simulations suggest that the clusters formed by **L²** and **L³** are more dynamic than the clusters formed by **L¹**. This is consistent with the reduction in intensity of the ions formed for higher order assemblies in the mass spectra for gold transport by **L²** and **L³** compared to **L¹**.

Recovery of gold and other metalates from mixed-metal solutions by L¹ – L³

The larger gold uptake seen when using **L²** and **L³** compared to **L¹** would also be expected when carrying out extractions from a *mixed-metal* solution representative of an acidic leach stream obtained from WEEE. As such, metal transport from a mixture of Cu(II), Al(III), Zn(II), Ni(II), Fe(III), Sn(IV) and Au(III) in 2 M HCl into separate toluene solutions of **L¹**, **L²** and **L³** (Figure 5) by solvent extraction was compared.

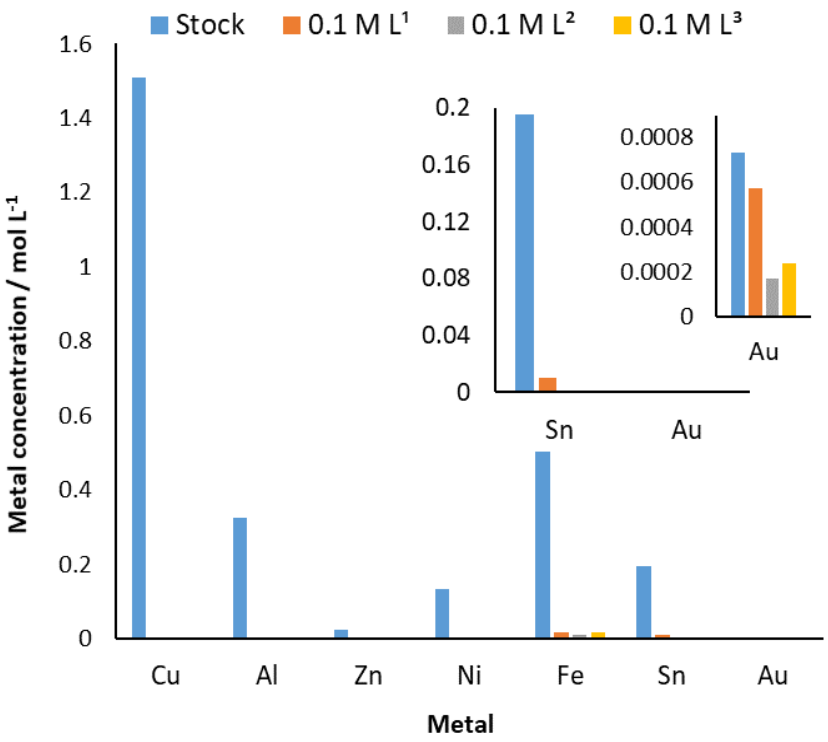

Figure 5. Concentration of metals transported into a toluene solution of **L**[1], **L**[2] or **L**[3] from a mixed-metal aqueous solution. Conditions: Solution of **L** (0.1 M) in toluene (2 mL) stirred (500 rpm) with mixed-metal solution (2 M HCl, 2 mL) for 1 h at RT.

As before,[32] the primary amide **L**[1] transports gold selectively into the organic phase at 78 %, with minimal co-extraction of Fe(III) (3 %) and Sn(IV) (5 %). In contrast, the 2° and 3° amides **L**[2] and **L**[3] transport markedly less gold than expected (23 % and 32 % respectively), and the other metals are also poorly transported. This lack of transport of any metal by **L**[2] and **L**[3] is surprising given the expected enhanced recovery of gold by the 2° and 3° amides over the 1° amide based on the gold-only study described above. However, inspection of the gold concentration in the raffinate showed that 76% and 81% of gold had been successfully removed from the mixed-metal feed by **L**[2] and **L**[3], respectively. Given this mass-balance discrepancy, a third phase was suspected to be forming but which could not be easily seen using small-scale (2 mL) solvent extraction

experiments. As such, the *mixed-metal* extraction experiments with **L**^{1}, **L**^{2} and **L**^{3} were up-scaled (20 mL:20 mL aqueous:organic) in order to quantify and characterize any 3rd phases.

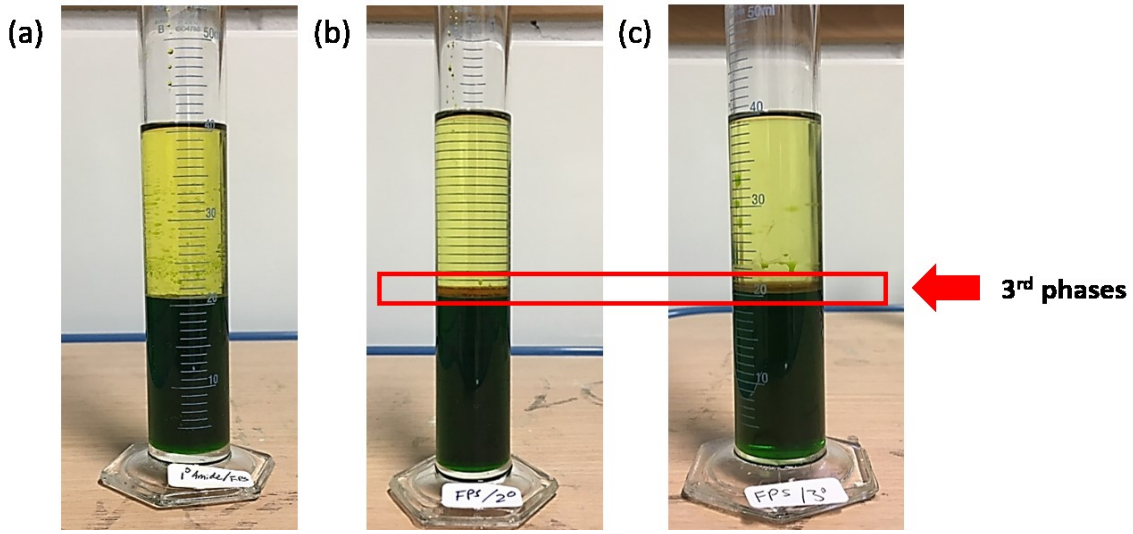

Figure 6. Photographs of the disengagement of organic (upper), 3rd phase (middle) and aqueous (lower) phases after contact of a 2 M HCl mixed-metal solution with 0.1 M toluene solutions of (a) **L**^{1} (no third phase), (b) **L**^{2} and (c) **L**^{3}.

While no 3rd phase was seen in extractions involving **L**^{1} upon scale-up, approximately 1 mL of a well-defined, viscous 3rd phase formed at the aqueous/organic interface in experiments with **L**^{2} and **L**^{3} (Figure 6). The 3rd phase for **L**^{2} comprises Au (2.8 %), Fe (87.6%), and Sn (9.6 %), representing almost 60% of the total Au available, but only 3% and 1% of Fe and Sn, respectively (Figure 7). The 3rd phase formed when using **L**^{3} comprises Au (1.4 %) and Fe (98.6 %) only, with all Sn remaining in the aqueous phase.

As Fe is the major constituent of these 3rd phases, an iron-absent *mixed-metal* aqueous solution was prepared to investigate if the presence of this metal was the trigger for 3rd phase formation. This proved to be the case for **L**^{3} as the Fe-free feed solution no 3rd phase is formed and 99% of the Au is extracted into the organic phase (Figure S6). In contrast, a 3rd phase remained is still

formed by **L²**, comprising 92% of the available Au and 15% Sn. Omission of both Fe and Sn from extractions by **L²** results in a 3rd phase comprising Zn, Cu, and Au. This result is particularly surprising given that zinc and copper metalates are not extracted to any significant extent from the single-metal aqueous solutions.

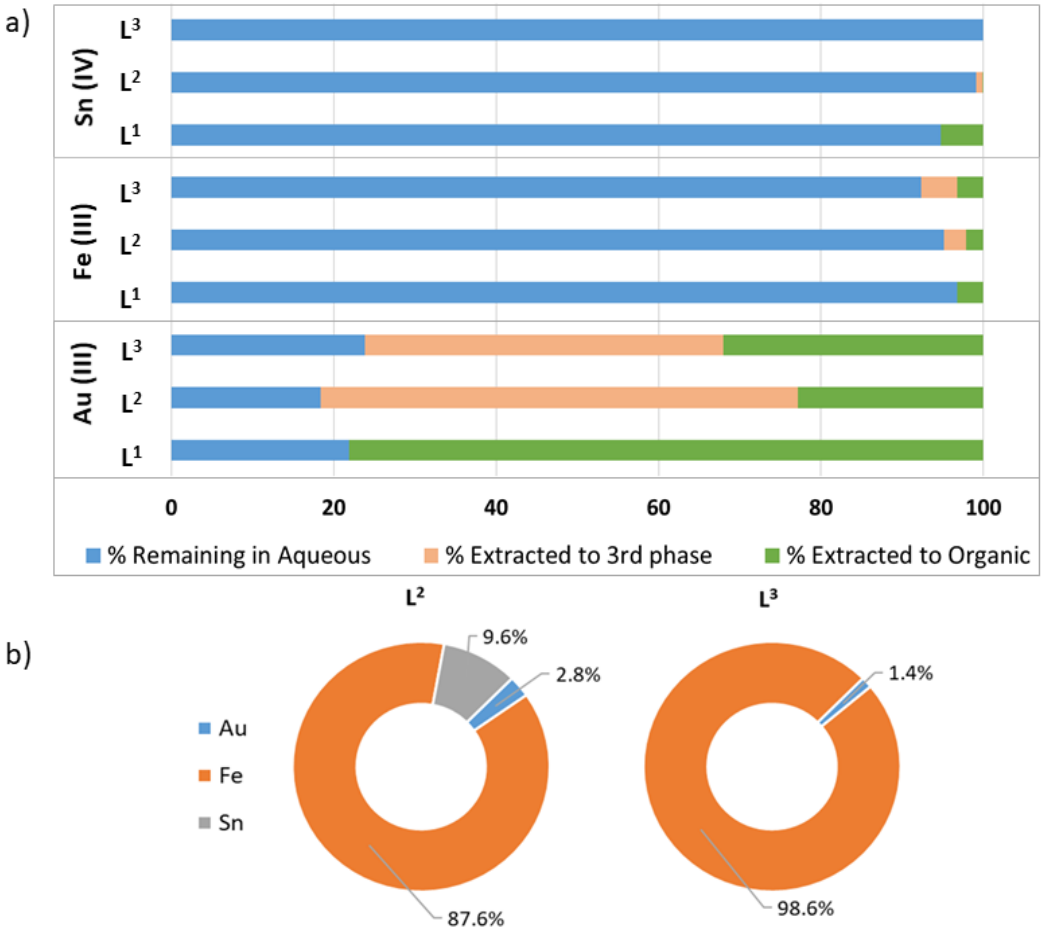

Figure 7. a) Percentage breakdown of metals transported by **L¹**, **L²** or **L³** into the 3rd phase, organic phase, or remaining in the aqueous phase. b) Breakdown of metal composition in the 3rd phases formed by **L²** and **L³**.

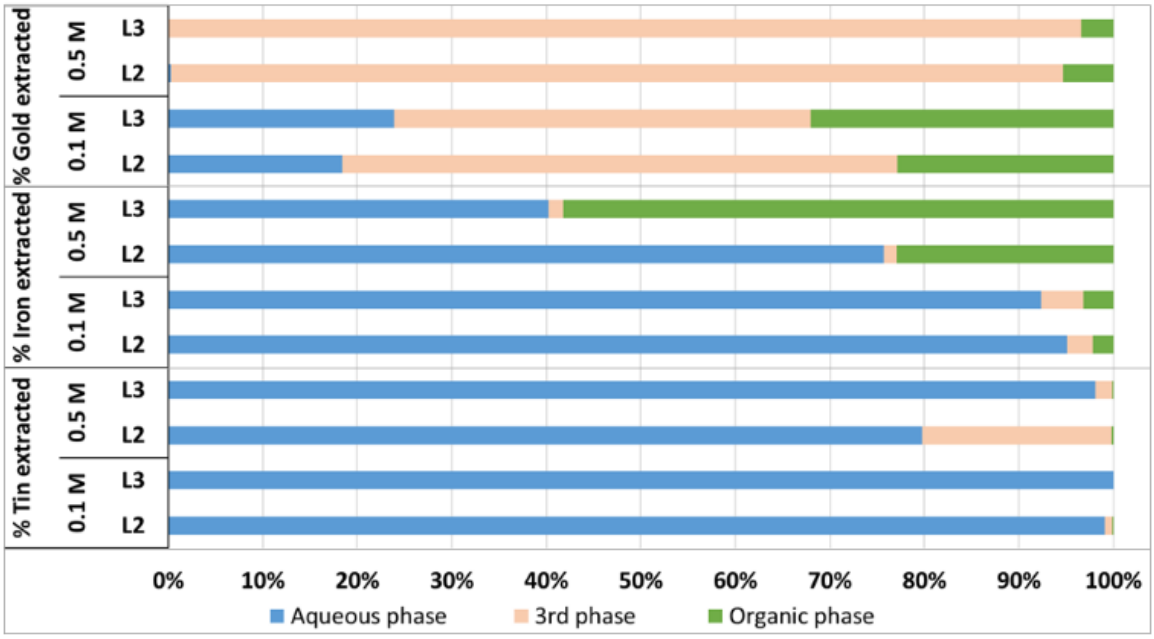

Figure 8. Comparison of the performance of the extractants $\mathbf{L^2}$ and $\mathbf{L^3}$ at different concentrations. Conditions: 0.1 M or 0.5 M **L** in toluene (20 mL) stirred (500 rpm) with a mixed-metal feed in 2 M HCl (20 mL) for 1 h at RT.

To discount any concentration differences between the single-metal and mixed-metal aqueous feeds, extractions with 0.5 M $\mathbf{L^2}$ and $\mathbf{L^3}$ were undertaken, resulting in approximately five times more of the third phase being formed (Figure 8). Interestingly, at these higher concentrations of reagent, more gold is extracted to the third phase, whilst iron is now transported to the organic phase. The secondary amide also extracted more tin when its concentration was increased to 0.5 M.

Third phase characterization and insights into mode of action.

During the experiments involving $\mathbf{L^3}$, colorless crystals formed at the aqueous/3rd phase interface which were isolated and studied by X-ray diffraction. The crystal data solve and refine as the octahedral dianionic metalate, $[SnCl_6]^{2-}$, charge-balanced by two protonated amide dimers $[H(\mathbf{L^3})_2]^+$ (Figure 9, top). In contrast to previous studies on amidoamine reagents where five-, six-

, and seven-membered intramolecular "proton chelates" form during metal transport,[31, 38-40] **L**^{3} instead forms a 2:1 assembly in which a proton is located between the amide oxygen atoms on neighboring molecules (O1---O2 2.426(2) Å), thus allowing charge-polarized C-H groups of the cation to interact with the charge-diffuse $[SnCl_6]^{2-}$ octahedron (Figure 9, bottom). These outer-sphere interactions reinforce the findings from the +ESI-MS spectra which showed that $[AuCl_4]^-$ ions remain intact to form clusters with the amides through outer-sphere interactions only.

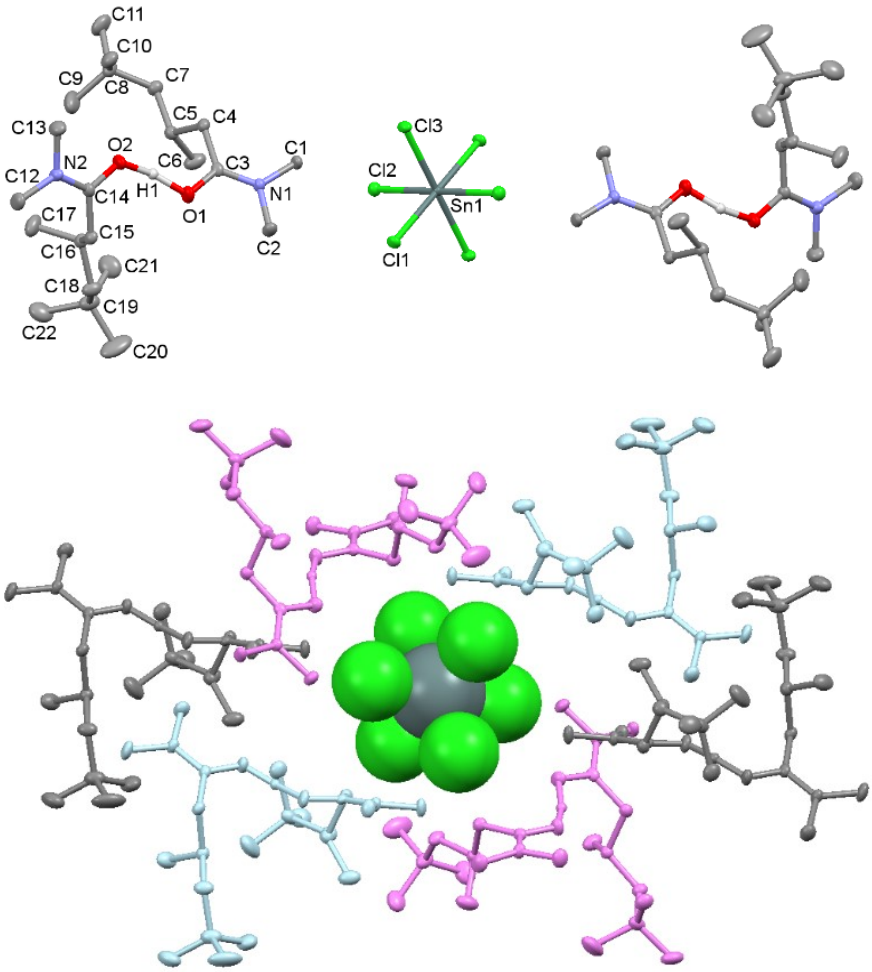

Figure 9. Solid-state structure of $[H(\mathbf{L}^{3})_2][SnCl_6]$. Top: $[SnCl_6]^{2-}$ charge-balanced by two $H(\mathbf{L}^{3})_2^{+}$ units. For clarity, all hydrogen atoms are omitted except H1 (displacement ellipsoids are drawn at 50% probability). Bottom: Space-filling model of $[SnCl_6]^{2-}$ encapsulated by six protonated dimers through CH---Cl interactions (colors show equivalent symmetries). Close contact distances (Å):

Cl1-C2 3.670(4); Cl1-C15 3.791(2); Cl2-C11 3.774(3); Cl3-C1 3.404(2); Cl3-C1' 3.628(2); Cl3-C4 3.863(2). Total of 6 C(H)---Cl interactions below 4.0 Å.

It is interesting that the solid-state structure of $[H(\mathbf{L^3})_2]_2[SnCl_6]$ does not contain water. This concurs with the ESI-MS data for the metal-loaded organic phases that do not contain peaks in which hydronium is present, and also with Karl-Fischer measurements that imply that little water is transported into the organic phase during metalate extraction. These conclusions are perhaps surprising as the amide is only weakly basic (pKa of protonated amides −0.3 to −1.2),[41] and consequently proton transfer from hydronium ion to the amide would be predicted to be unfavorable. Significantly, recent analysis of organic-phase ion-pair structures in solvent extraction experiments has shown that microhydration likely provides a pathway for enhanced thermodynamic stability of these structures through increased hydrogen-bonding interactions.[42-43] The exchange of N-H protons in organic amides is well studied due to its use as a method to understand the number and types of accessible amides in folded proteins.[44] Proton exchange in amides can be acid- or base-catalyzed, with mechanisms for the acid-catalyzed pathway following either O- or N-protonation, with a strong tendency for initial amide-O protonation.[45] Importantly, the protonation of amides has been studied by computational modelling,[46-47] with gas-phase calculations providing a good approximation of the non-polar environment of the organic phase in a solvent extraction experiment,[34] and the incorporation of a polar solvent continuum model approximating the aqueous phase. In the gas phase, spontaneous proton transfer from hydronium to the O-atom of the amide was favored by 30 kcal mol^{-1}, whereas in a polar solvent environment this reduced to 2.5 kcal mol^{-1}. As such, it is apparent that amides $\mathbf{L^1}$-$\mathbf{L^3}$ may become protonated at the amide O-atom in the organic phase, and that water, other than that implicit to the hydrated solvent, may not play a significant role in the assembly of the aggregated gold structures.

Attempts to characterize the liquid 3rd phases proved more difficult. ESI-MS studies show only ions of complex clusters comprising "FeCl" with varying proportions of **L** (Figures S7 and S8). Since the 3rd phases contain iron (which is paramagnetic), simple NMR experiments proved inconclusive. However, DOSY ^{1}H NMR analysis of the third phase formed between 0.1 M $\mathbf{L^2}$ (in d_6-benzene) and an Fe-absent mixed-metal feed (all other transported metals were diamagnetic) shows a broad peak correlating to the $\mathbf{L^2}$ alkyl chain with a diffusion rate much slower than benzene solvent (Figure S9 a); this is consistent with the presence of a viscous, potentially polymeric phase. In addition, all loaded organic phases display similar DOSY spectra to their analogous uncontacted organic phases, diffusing faster than the third phase and therefore are less aggregated. Diluting the 3rd phase in more polar solvents such as deuterated methanol (MeOD) results in a DOSY spectrum (Figure S9 c) similar to those of the uncontacted ligand (Figure S9 d) and the organic phase (Figure S9 b), suggesting the more polar solvents disrupt the molecular aggregation.

The ^{1}H NMR spectrum of a 3rd phase derived from $\mathbf{L^2}$ formed after contact with the iron-absent mixed-metal solution in MeOD, displays a singlet at 4.87 ppm that is consistent with water (Figure S9 c). Consequently, the concentrations of water in the 3rd phases were determined by Karl-Fischer analyses and compared with those of the organic phases (Table 2). The water content in an organic phase of $\mathbf{L^1}$ loaded from the *mixed-metal* feed was *ca*. 300 ppm higher than that seen for an organic phase loaded solely from a single Au solution.[32] The metal-loaded 3rd phases have around five times more water than the metal-loaded organic phases, which may explain lack of solubility of the third phase. The concentrations of amide reagent in the 3rd phase were also determined by calibrated ^{1}H NMR spectroscopy. In these cases, it is found that the approximate concentration of the amide $\mathbf{L^3}$ in a water-stripped 3rd phase is 1.15 mol L^{-1} whereas the loaded organic phase is just

0.04 mol L^{-1} (Table 2), i.e. the 3rd phase incorporates a significant quantity of the amide reagent. Loss of the amides into the 3rd phase points to potential aggregation between **L³**, Fe(III) and Au(III) and water. As described earlier, diminished clustering by **L²** and **L³** compared with **L¹** (which does not form a 3rd phase) may result in hydrogen-bonded clusters which are more porous, and hence are more able to aggregate into more extended, and dense, structures.[48-49]

Table 2. Concentrations of amide and water determined for organic and third phases.

Sample[a]	Amide (mol L^{-1})[b]	Water (ppm)[c]	Water (mol L^{-1})[c]
Uncontacted organic phase **L¹**	0.10	209	0.012
Loaded organic phase **L¹**	0.07	746	0.041
Uncontacted organic phase **L²**	0.10	273	0.015
Loaded organic phase **L²**	0.03	456	0.025
3rd phase **L²**	1.67	1064	0.059
Uncontacted organic phase **L³**	0.11	202	0.011
Loaded organic phase **L³**	0.04	453	0.025
3rd phase **L³**	1.15	993	0.055

[a] Samples taken from amide solutions in benzene. [b] Determined in triplicate by ^{1}H NMR concentration using 1,4-dioxane as an internal standard; for amide concentrations the metal-loaded organic phase was back-extracted with H_2O prior to NMR analysis to avoid interference by paramagnetic Fe(III). [c] Determined in triplicate by volumetric Karl-Fischer titration.

With the exception of omitting Fe from the solvent extraction experiment using **L³**, omission of any other metal failed to negate 3rd phase formation using either **L²** or **L³**. As aggregation is not observed by DOSY NMR spectroscopy when sampling the third phase in more polar solvents, solvent extraction experiments with 0.1 M **L²** or **L³** solutions in chloroform or 10% (v/v) 1-octanol in toluene were carried out. In these cases, no 3rd phase formation is seen with almost quantitative transport of Au into the organic phase occurring for both **L²** and **L³**, albeit with a loss of selectivity

compared with **L**[1] with increased amounts of Sn (6-8%) and Fe (11-16%) extracted (Figure 10). It is likely that the enhanced polarity and hydrogen-bonding ability of these solvents compared to toluene could be the deconstructing aggregates formed in the 3rd phase.

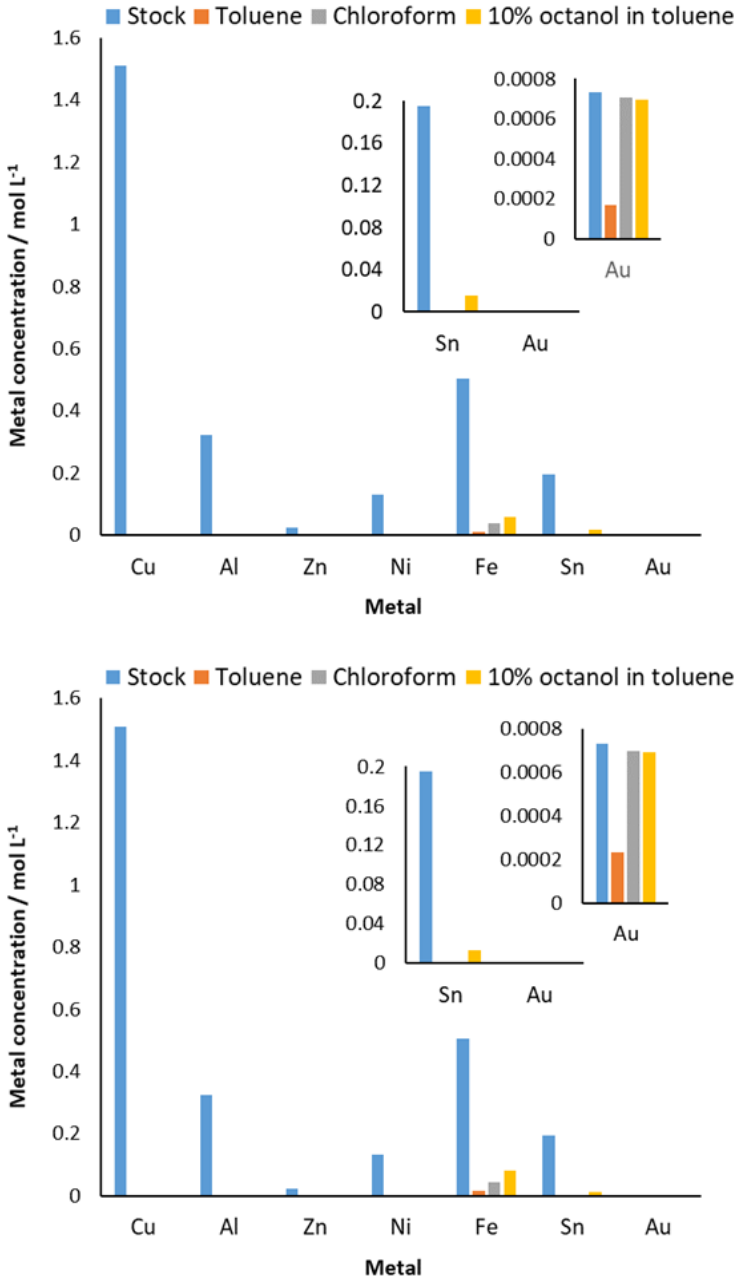

Figure 10. Concentration of metals loaded into toluene, chloroform, or toluene/octanol (10%) organic phases of **L**[2] (top) or **L**[3] (bottom) from a mixed-metal aqueous solution. Conditions: 0.1

M **L** in 10 % (v/v) octanol in toluene (2 mL) or chloroform (2 mL) stirred (500 rpm) with a mixed-metal feed in 2 M HCl (2 mL) for 1 h at RT.

CONCLUSIONS

Secondary and tertiary analogues (**L²** and **L³**) of a simple primary amide (**L¹**) have been shown to be excellent at transporting monoanionic chloridometalates from acidic single-metal solutions into a hydrophobic organic phase. As expected,[35-36] the strength of this transport by solvent extraction follows the order 3° > 2° > 1°. The chemical mechanism of transport of $AuCl_4^-$ has been studied and it follows that protonation of the amides occurs, forming charge-diffuse receptors that display an enhanced preference to interact with the charge-diffuse monoanionic metalates than with the charge-localized chloride present in excess. Computational modelling suggests that the propensity of the amide series to form discrete clusters with multiple $AuCl_4^-$ ions diminishes as the N–H donor sites are removed from the reagent, and this, along with the amide basicity, provides a rationale to the strength of extraction.

While the single-metal experiments show that the 2° and 3° amides should transfer gold more effectively from a mixed-metal aqueous solution representative of WEEE to the organic phase, this is not the case as gold-concentrated third phases form when iron and tin are in high concentrations with **L²** and when iron is present with **L³**. Exclusion of iron from the mixed-metal solution prevents third phase formation by **L³**, but the issue persists with **L²**. Third-phase formation can be circumvented by increasing the polarity of the less-polar phase using chloroform or by adding a modifier such as 1-octanol, albeit with a decrease in selectivity of separation. As such, the exploitation of these secondary and tertiary amides in gold recovery from WEEE by solvent extraction will depend strongly on the identity of the metals present in the WEEE feed stream. Also, losses of the amide reagents to the third phase and in some cases to the aqueous phase are

potential challenges. However, the ease of synthesis of these compounds from inexpensive and commercially available materials, and their strength and selectivity compared with other amide reagents are advantageous.

The ability of the primary amide to promote the formation of molecular hydrophobic assemblies through the availability of hydrogen-bond donors and acceptors appears crucial to its success in metalate separation by solvent extraction. These groups are diminished in the secondary and tertiary amides which likely causes third-phase formation and which is only circumvented by the use of more-polar, hydrogen-bonding diluents. It is also interesting that water does not appear necessary to stabilize the structures of the molecular clusters seen in the organic phase, at least in the case of $[H(\mathbf{L^3})_2]_2[SnCl_6]$, but clearly this may not be the case for other metal species; the proton necessary for charge-balance of the ion pair in $[H(\mathbf{L^3})_2]_2[SnCl_6]$ is solely solvated by intermolecular hydrogen-bonding interactions with the O-donor atoms of the amides. This latter feature is similar to that seen previously in the extraction of anions by amidoamines,[31, 38-40] and is supported by computational modelling of proton transfer between hydronium ions and amides.[46-47] However, this contrasts to recent work that showed that some lanthanide complexes and nitratometalates in the organic phase are microhydrated[50-52] by defined amounts of water which acts as a supramolecular structural motif.[42-43] While these solvent extraction mechanisms appear to have some similarities, it is clear that further experimental and computational studies are required to understand the significance of microhydration to the stability of metal complexes and assemblies that form in the organic phase and their relevance to the separation of metals by solvent extraction.

EXPERIMENTAL

Materials and instruments. All solvents and reagents were used as received from Sigma-Aldrich, Fisher Scientific UK, Alfa Aesar, Acros Organics or VWR International. Deionised water was obtained from a Milli-Q purification system. The amide **L^1** was prepared according to the literature synthesis.[32] All NMR spectra were recorded at 300 K unless otherwise stated. ^{1}H and ^{13}C spectra were recorded on a Bruker AVA500 spectrometer (^{1}H: 500.12, ^{13}C: 125.76 MHz). Elemental analyses were carried out by Stephen Boyer at the London Metropolitan University Elemental Analysis Service (London Metropolitan University, School of Human Sciences, Science Centre, 29 Hornsey Road, London, N7 7DD). ESI FT-ICR MS measurements were recorded in positive-ion mode using the standard Bruker ESI sprayer operated in "infusion" mode coupled to a SolariX FTICR mass spectrometer. Direct infusion spectra were typically a sum of 20 acquisitions. All mass spectra were analysed using DataAnalysis software version 4.1 SR1 build 362.7 (Bruker Daltonics). Ions were assigned manually. ICP-OES analysis was carried out on a Perkin Elmer Optima 5300DC Inductively Coupled Plasma Optical Emission Spectrometer. Samples in 1-methoxy-2-propanol were taken up by peristaltic pump at a rate of 2.0 mL min^{-1} into a Gem Tip cross flow nebuliser and a glass cyclonic spray chamber. Argon plasma conditions were: 1500 W RF forward power, argon gas flows of 20, 1.4 and 0.45 L min^{-1} for plasma, auxiliary and nebuliser flow, respectively. ICP-OES calibration standards were obtained from VWR International or Sigma-Aldrich.

Syntheses S1 of L^1 (see ref. 32), L^2, and L^3

N,3,5,5-tetramethylhexanamide, L^2. 3,5,5-trimethylhexanoyl chloride (10 mL, 0.053 mol) was added dropwise to an aqueous methylamine solution (100 mL, 40 wt%) at 0 °C, and was stirred overnight at room temperature. The crude product was extracted into dichloromethane (100 mL)

and washed with water (3 x 80 mL). The organic phase was dried over Na_2SO_4 and the solvent removed under reduced pressure to give the title compound as a colourless oil (8.07 g, 89 %).

^{1}H NMR (500 MHz, $CDCl_3$) δ: 6.32 (s, 1H, N*H*), 2.74 (d, 3H, N(C*H*$_3$)), 2.15 (dd, 1H, C*H*$_2$CO *J* =13.6, 5.9 Hz), 2.08 – 1.96 (m, 1H, C*H*(CH$_3$)), 1.92 (dd, 1H, C*H*$_2$CO *J* = 13.6, 8.3 Hz), 1.19 (dd, 1H, C*H*$_2$C(CH$_3$)$_3$ *J* = 14.0, 3.9 Hz), 1.05 (dd, 1H, C*H*$_2$C(CH$_3$)$_3$ *J* = 14.0, 6.6 Hz), 0.91 (d, 3H, CH(C*H*$_3$) *J* = 6.6 Hz), 0.85 (s, 9H, C(C*H*$_3$)$_3$).

^{13}C NMR (126 MHz, $CDCl_3$) δ: 173.42, 50.69, 46.39, 30.98, 29.95, 27.34, 26.08, 22.56.

^{1}H NMR (500 MHz, C_6D_6, ppm) δ = 6.16 (s, 1H, N*H*), 2.60 (d, 3H, N(C*H*$_3$) *J* = 4.7 Hz), 2.27 – 2.18 (m, 1H, C*H*(CH$_3$)), 2.12 (dd, 1H, C*H*$_2$CO *J* = 13.9, 6.1 Hz), 1.89 (dd, 1H, C*H*$_2$CO *J* = 13.9, 8.2 Hz), 1.29 (dd, 1H, C*H*$_2$C(CH$_3$)$_3$ *J* = 14.0, 3.9 Hz), 1.08 (dd, 1H, C*H*$_2$C(CH$_3$)$_3$ *J* = 14.0, 6.6 Hz), 1.01 (d, 3H, CH(C*H*$_3$) *J* = 6.7 Hz), 0.92 (s, 9H, C(C*H*$_3$)$_3$).

^{13}C NMR (126 MHz, C_6D_6, ppm) δ: 172.42, 50.71, 46.09, 30.81, 29.84, 27.23, 25.69, 22.64.

ESI-MS (m/z) $C_{10}H_{21}NO$ $[M+H]^+$, calcd. 172.169, found 172.169.

N,N,3,5,5-pentamethylhexanamide, L^3. 3,5,5-trimethylhexanoyl chloride (10 mL, 0.053 mol) was added dropwise to an aqueous dimethylamine solution (100 mL, 40 wt%) at 0 °C, and was stirred overnight at room temperature. The crude product was extracted into dichloromethane (100 mL) and washed with water (3 x 80 mL). The organic phase was dried over Na_2SO_4 and the solvent removed under reduced pressure to give the title compound as a colourless oil (8.34 g, 85 %).

^{1}H NMR (500 MHz, $CDCl_3$) δ: 2.94 (s, 3H, N(C*H*$_3$)), 2.87 (s, 3H, N(C*H*$_3$)), 2.20 (dd, 1H, C*H*$_2$CO *J* = 14.6, 5.7 Hz), 2.11 (dd, 1H, C*H*$_2$CO *J* = 14.6, 8.2), 2.08 – 1.99 (m, 1H, C*H*(CH$_3$)), 1.22 (dd, 1H, C*H*$_2$C(CH$_3$)$_3$ *J* = 14.0, 3.8 Hz), 1.05 (dd, 1H, C*H*$_2$C(CH$_3$)$_3$ *J* = 14.0, 6.5 Hz), 0.91 (d, 3H, CH(C*H*$_3$) *J* = 6.5 Hz), 0.84 (s, 9H, C(C*H*$_3$)$_3$).

^{13}C NMR (126 MHz, $CDCl_3$) δ: 172.50, 50.84, 42.72, 37.41, 35.25, 31.04, 29.95, 26.84, 22.83.

^{1}H NMR (500 MHz, C_6D_6, ppm) δ: 2.66 (s, 3H, N(CH_3)), 2.28 (s, 3H, N(CH_3)), 2.27 – 2.22 (m, 1H, CH(CH_3)), 2.04 (dd, 1H, CH_2CO J = 15.1, 5.8 Hz), 1.91 (dd, 1H, CH_2CO J = 15.1, 8.0 Hz), 1.30 (dd, 1H, CH_2C(CH_3)$_3$ J = 13.8, 3.9 Hz), 1.05 (dd, 1H, CH_2C(CH_3)$_3$ J = 13.8, 3.9 Hz), 1.02 (d, 3H, CH(CH_3) J = 6.6 Hz), 0.92 (s, 9H, C(CH_3)$_3$).

^{13}C NMR (126 MHz, C_6D_6, ppm) δ: 170.95, 50.90, 42.56, 36.14, 34.58, 30.88, 29.88, 26.63, 22.95.

ESI-MS (m/z) $C_{11}H_{23}NO$ $[M+H]^+$, calcd. 186.185, found 186.1853.

Solvent extraction procedures

1. Extractions of metals from single-metal solutions of varying concentrations of aqueous HCl into toluene using amides L. The extractions were carried out using 0.01 M of the metal salt dissolved in varying concentrations of HCl (2 mL, 0-12 M) that were contacted with 0.1 M of **L** in toluene (2 mL) at 20 ºC for 1 h with magnetic stirring. The concentrations of metals extracted into the organic phase were determined using ICP-OES by appropriate dilution of the solution into 1-methoxy-2-propanol.

2. Extractions of Au into varying concentrations of amide L in toluene from an aqueous $AuCl_4^-$ solution of constant [HCl]. The extractions were carried out using 0.01 M of $HAuCl_4$ dissolved in HCl (2 mL, 6 M) that were contacted with varying concentrations of **L** (0.001 – 0.100 M) in toluene (2 mL) at 20 ºC for 1 h with magnetic stirring. The concentrations of gold extracted into the organic phase were determined using ICP-OES by appropriate dilution of the solution into 1-methoxy-2-propanol.

3. Extractions of metals from an aqueous mixed-metal feed, representative of the concentrations of metals found in a standard mobile phone, into toluene using amides L. The extractions were carried out using an aqueous mixed-metal solution (containing Cu 1.5; Al 0.35; Zn 0.03; Ni 0.15; Fe 0.5; Sn 0.20; Au 0.001 mol L^{-1}) dissolved in HCl (2 mL, 2 M) that were

contacted with 2 mL of 0.1 amide **L** solution at 20 ºC for 1 h with magnetic stirring. The concentrations of metals extracted into the organic phase were determined using ICP-OES by appropriate dilution of the solution into 1-methoxy-2-propanol.

Computational methods. Geometry optimization calculations were carried out for **L**, **L**H^+ and $AuCl_4^-$ in various combinations using the Gaussian 09 program.[53] The dispersion-corrected M06 exchange/correlation functional was used throughout,[54] due to the importance of dispersion correction in accurately predicting the strength of non-covalent interactions, which play a key role in the proposed mode of action of the extractant investigated in this study. The LANL2DZ pseudopotential/basis set was used for gold,[55] with the 6-31+G* basis set being used for all other atoms. Structures were considered optimized when the forces and atomic displacements fell to within the program default convergence criteria. Classical molecular dynamics (MD) simulations were employed using the OPLS-AA force field with the software package LAMMPS.[56] For each of amides **L**^{1}-**L**^{3}, three initial geometries, comprising four **L**H^+, six **L**, and four $AuCl_4^-$ entities randomly distributed in a cubic simulation cell of length 60 Å, were constructed using Packmol. For $AuCl_4^-$ atomic charges were assigned as -0.25 on each of the chlorine atoms, zero on the Au, Au–Cl = 2.39 Å, ∠Cl–Au–Cl = 90°, with force constants of 400 kcal mol^{-1} Å^{-2} and 50 kcal mol^{-1} deg^{-2}, respectively. From each starting geometry, simulations were run under isothermal-isobaric (NPT) ensemble conditions, following a short equilibration period under canonical (NVT) ensemble conditions. Simulations were conducted at temperatures of 298 K, using the Nosé-Hoover thermostat system to maintain constant temperature. The integration time step was set to 1 fs, and time increments accrued using the standard Velocity-Verlet algorithm. In total, system dynamics were accrued for 10.2 ns, including 500 ps equilibration time. In each frame of each simulation, the number of amide nitrogen atoms within a distance of 4 Å of at least one chlorine

atom was counted. The total count over all frames of a simulation was divided by the theoretical maximum value (i.e. the number of frames in the simulation multiplied by 10) and multiplied by 100 to give the average percentage of nitrogen atoms within the threshold distance of a chlorine atom at any given point in the simulation.

X-ray Crystallography. Data were collected at 120.01(10) K on an Oxford Diffraction Excalibur diffractometer equipped with an Eos CCD detector using graphite-monochromated Mo-K radiation ($\lambda = 0.71073$ Å). Structures were solved using ShelXT direct methods or intrinsic phasing and refined using a full-matrix least square refinement on $|F|^2$ using ShelXL.[57] All programs were used within the Olex suites.[58] All non-hydrogen atoms refined with anisotropic displacement parameters. H-atom parameters were constrained to parent atoms and refined using a riding model except H1 which was located in the difference Fourier map and refined with isotropic displacement parameters.

ASSOCIATED CONTENT

Supporting Information.

The following file is available free of charge.

Supporting Information, Figures S1-S12 and Tables S1-S3 (PDF)

AUTHOR INFORMATION

Corresponding Author

*email: jason.love@ed.ac.uk

Present Addresses

†Imperial College London, Department of Chemistry, London SW7 2AZ, UK.

Author Contributions

The manuscript was written through contributions of all authors. All authors have given approval to the final version of the manuscript.

Funding Sources

Natural Environment Research Council for a PhD studentship through the E3 DTP (L. M. M. K., grant number NE/L002558/1).

ACKNOWLEDGMENT

The authors thank the School of Chemistry at the University of Edinburgh for funding, access to analytical facilities, and the funding of a Principal's Career Development Scholarship (E. D. D.), the Edinburgh Computer and Data Facility for access to high-performance computing, and the Natural Environment Research Council for a PhD studentship through the E3 DTP (L. M. M. K., grant number NE/L002558/1).

REFERENCES

1. Berners-Price, S. J.; Filipovska, A., Gold compounds as therapeutic agents for human diseases. *Metallomics* **2011,** *3* (9), 863-873.

2. Hughes, M. D.; Xu, Y.-J.; Jenkins, P.; McMorn, P.; Landon, P.; Enache, D. I.; Carley, A. F.; Attard, G. A.; Hutchings, G. J.; King, F.; Stitt, E. H.; Johnston, P.; Griffin, K.; Kiely, C. J., Tunable gold catalysts for selective hydrocarbon oxidation under mild conditions. *Nature* **2005,** *437* (7062), 1132-1135.

3. Hutchings, G., A golden future. *Nat Chem* **2009,** *1* (7), 584-584.

4. Pérez-López, A. M.; Rubio-Ruiz, B.; Sebastián, V.; Hamilton, L.; Adam, C.; Bray, T. L.; Irusta, S.; Brennan, P. M.; Lloyd-Jones, G. C.; Sieger, D.; Santamaría, J.; Unciti-Broceta, A., Gold-Triggered Uncaging Chemistry in Living Systems. *Angew. Chem. Int. Ed.* **2017,** *56* (41), 12548-12552.

5. Hagelüken, C.; Corti, C. W., Recycling of gold from electronics: cost-effective use through 'design for recycling'. *Gold Bulletin* **2010,** *43*, 209-220.

6. UNEP *Recycling - From E-waste to resources*; July 2009.

7. Bigum, M.; Brogaard, L.; Christensen, T. H., Metal recovery from high-grade WEEE: A life cycle assessment. *J. Hazard. Mater.* **2012,** *207–208*, 8-14.

8. Ding, Y.; Zhang, S.; Liu, B.; Zheng, H.; Chang, C.-c.; Ekberg, C., Recovery of precious metals from electronic waste and spent catalysts: A review. *Resour. Conserv. Recy.* **2019,** *141*, 284-298.

9. Nelson, J. J. M.; Schelter, E. J., Sustainable Inorganic Chemistry: Metal Separations for Recycling. *Inorg. Chem.* **2019,** *58* (2), 979-990.

10. Rigoldi, A.; Trogu, E. F.; Marcheselli, G. C.; Artizzu, F.; Picone, N.; Colledani, M.; Deplano, P.; Serpe, A., Advances in Recovering Noble Metals from Waste Printed Circuit Boards (WPCBs). *ACS Sustainable Chem. Eng.* **2019,** *7* (1), 1308-1317.

11. Velenturf, A. P. M.; Jopson, J. S., Making the business case for resource recovery. *Sci. Total Environ.* **2019,** *648*, 1031-1041.

12. Sholl, D. S.; Lively, R. P., Seven chemical separations to change the world. *Nature* **2016,** *532*, 435-437.

13. Weisz, H.; Suh, S.; Graedel, T. E., Industrial Ecology: The role of manufactured capital in sustainability. *Proc. Nat. Acad. Sci.* **2015,** *112* (20), 6260-6264.

14. Syed, S., Recovery of gold from secondary sources—A review. *Hydrometallurgy* **2012,** *115–116*, 30-51.

15. Love, J. B.; Miguirditchian, M.; Chagnes, A., New Insights into the Recovery of Strategic and Critical Metals by Solvent Extraction: The Effects of Chemistry and the Process on Performance. In *Ion Exchange and Solvent Extraction: Changing the Landscape in Solvent Extraction*, Moyer, B. A., Ed. CRC Press: 2019; Vol. 23.

16. Räisänen, M.; Heliövaara, E.; Al-Qaisi, F. a.; Muuronen, M.; Eronen, A.; Liljeqvist, H.; Nieger, M.; Kemell, M.; Moslova, K.; Hämäläinen, J.; Lagerblom, K.; Repo, T., Pyridinethiol-Assisted Dissolution of Elemental Gold in Organic Solutions. *Angew. Chem. Int. Ed.* **2018,** *57* (52), 17104-17109.

17. Yue, C.; Sun, H.; Liu, W.-J.; Guan, B.; Deng, X.; Zhang, X.; Yang, P., Environmentally Benign, Rapid, and Selective Extraction of Gold from Ores and Waste Electronic Materials. *Angew. Chem. Int. Ed.* **2017,** *56* (32), 9331-9335.

18. Foley, S.; Salimi, H. Methods for simultaneous leaching and extraction of precious metals. US Patent WO2016168930A1, 2016.

19. Jadhav, U.; Hocheng, H., Hydrometallurgical Recovery of Metals from Large Printed Circuit Board Pieces. *Sci. Rep.* **2015,** *5*, 14574.

20. Do, J.-L.; Tan, D.; Friščić, T., Oxidative Mechanochemistry: Direct, Room-Temperature, Solvent-Free Conversion of Palladium and Gold Metals into Soluble Salts and Coordination Complexes. *Angew. Chem. Int. Ed.* **2018,** *57* (10), 2667-2671.

21. Jovanovič, P.; Šelih, V. S.; Šala, M.; Hodnik, N., In situ electrochemical dissolution of platinum and gold in organic-based solvent. *npj Materials Degradation* **2018,** *2* (1), 9.

22. Kubota, F.; Kono, R.; Yoshida, W.; Sharaf, M.; Kolev, S. D.; Goto, M., Recovery of gold ions from discarded mobile phone leachate by solvent extraction and polymer inclusion membrane (PIM) based separation using an amic acid extractant. *Sep. Purif. Technol.* **2019,** *214*, 156-161.

23. Sun, D. T.; Gasilova, N.; Yang, S.; Oveisi, E.; Queen, W. L., Rapid, Selective Extraction of Trace Amounts of Gold from Complex Water Mixtures with a Metal–Organic Framework (MOF)/Polymer Composite. *J. Am. Chem. Soc.* **2018,** *140* (48), 16697-16703.

24. Lahtinen, E.; Kivijärvi, L.; Tatikonda, R.; Väisänen, A.; Rissanen, K.; Haukka, M., Selective Recovery of Gold from Electronic Waste Using 3D-Printed Scavenger. *ACS Omega* **2017,** *2* (10), 7299-7304.

25. Wu, Y.; Fang, Q.; Yi, X.; Liu, G.; Li, R.-W., Recovery of gold from hydrometallurgical leaching solution of electronic waste via spontaneous reduction by polyaniline. *Prog. Nat. Sci.: Mater. Int.* **2017,** *27* (4), 514-519.

26. Liu, Z.; Frasconi, M.; Lei, J.; Brown, Z. J.; Zhu, Z.; Cao, D.; Iehl, J.; Liu, G.; Fahrenbach, A. C.; Botros, Y. Y.; Farha, O. K.; Hupp, J. T.; Mirkin, C. A.; Fraser Stoddart, J., Selective isolation of gold facilitated by second-sphere coordination with α-cyclodextrin. *Nat. Commun.* **2013,** *4*, 1855.

27. Pati, P.; McGinnis, S.; Vikesland, P. J., Waste not want not: life cycle implications of gold recovery and recycling from nanowaste. *Environ. Sci., Nano.* **2016,** *3* (5), 1133-1143.

28. Wilson, A. M.; Bailey, P. J.; Tasker, P. A.; Turkington, J. R.; Grant, R. A.; Love, J. B., Solvent extraction: the coordination chemistry behind extractive metallurgy. *Chem. Soc. Rev.* **2014,** *43* (1), 123-134.

29. Izatt, R. M.; Izatt, S. R.; Bruening, R. L.; Izatt, N. E.; Moyer, B. A., Challenges to achievement of metal sustainability in our high-tech society. *Chem. Soc. Rev.* **2014,** *43* (8), 2451-2475.

30. Rydberg, J.; Cox, M.; Musikas, C.; Choppin, G. R., *Principles and practices of solvent extraction*. 2nd ed.; Marcel Dekker: New York, 2004; p 584.

31. Turkington, J. R.; Bailey, P. J.; Love, J. B.; Wilson, A. M.; Tasker, P. A., Exploiting outer-sphere interactions to enhance metal recovery by solvent extraction. *Chem. Commun.* **2013,** *49* (19), 1891-1899.

32. Doidge, E. D.; Carson, I.; Tasker, P. A.; Ellis, R. J.; Morrison, C. A.; Love, J. B., A Simple Primary Amide for the Selective Recovery of Gold from Secondary Resources. *Angew. Chem. Int. Ed.* **2016,** *55* (40), 12436-12439.

33. Preston, J. S.; du Preez, A. C., Solvent extraction of uranium(VI) and thorium(IV) from nitrate media by carboxylic acid amides. *Solvent Extr. Ion Exch.* **1995,** *13* (3), 391-413.

34. Carson, I.; MacRuary, K. J.; Doidge, E. D.; Ellis, R. J.; Grant, R. A.; Gordon, R. J.; Love, J. B.; Morrison, C. A.; Nichol, G. S.; Tasker, P. A.; Wilson, A. M., Anion Receptor Design:

Exploiting Outer-Sphere Coordination Chemistry To Obtain High Selectivity for Chloridometalates over Chloride. *Inorg. Chem.* **2015,** *54* (17), 8685-8692.

35. Mowafy, E. A.; Mohamed, D., Extraction and separation of gold(III) from hydrochloric acid solutions using long chain structurally tailored monoamides. *Sep. Purif. Technol.* **2016,** *167*, 146-153.

36. Narita, H.; Tanaka, M.; Morisaku, K.; Abe, T., Extraction of gold(III) in hydrochloric acid solution using monoamide compounds. *Hydrometallurgy* **2006,** *81* (3–4), 153-158.

37. Habashi, F., *A Textbook of Hydrometallurgy, 2nd edition*. Métallurgie Extractive Québec: Quebec, 1999; Vol. 13.

38. Cokoja, M.; Markovits, I. I. E.; Anthofer, M. H.; Poplata, S.; Pöthig, A.; Morris, D. S.; Tasker, P. A.; Herrmann, W. A.; Kühn, F. E.; Love, J. B., Catalytic epoxidation by perrhenate through the formation of organic-phase supramolecular ion pairs. *Chem. Commun.* **2015,** *51* (16), 3399-3402.

39. Ellis, R. J.; Chartres, J.; Henderson, D. K.; Cabot, R.; Richardson, P. R.; White, F. J.; Schröder, M.; Turkington, J. R.; Tasker, P. A.; Sole, K. C., Design and Function of Pre-organised Outer-Sphere Amidopyridyl Extractants for Zinc(II) and Cobalt(II) Chlorometallates: The Role of C□H Hydrogen Bonds. *Chem. Eur. J.* **2012,** *18* (25), 7715-7728.

40. Turkington, J. R.; Cocalia, V.; Kendall, K.; Morrison, C. A.; Richardson, P.; Sassi, T.; Tasker, P. A.; Bailey, P. J.; Sole, K. C., Outer-Sphere Coordination Chemistry: Amido-Ammonium Ligands as Highly Selective Tetrachloridozinc(II)ate Extractants. *Inorg. Chem.* **2012,** *51* (23), 12805-12819.

41. Grant, H.; Mctigue, P.; Ward, D., The basicities of aliphatic amides. *Aust. J. Chem.* **1983,** *36* (11), 2211-2218.

42. Baldwin, A. G.; Ivanov, A. S.; Williams, N. J.; Ellis, R. J.; Moyer, B. A.; Bryantsev, V. S.; Shafer, J. C., Outer-Sphere Water Clusters Tune the Lanthanide Selectivity of Diglycolamides. *ACS Cent. Sci.* **2018,** *4* (6), 739-747.

43. Hunter, J. P.; Dolezalova, S.; Ngwenya, B. T.; Morrison, C. A.; Love, J. B., Understanding the Recovery of Rare-Earth Elements by Ammonium Salts. *Metals* **2018,** *8* (6), 465.

44. Perrin, C. L., Proton exchange in amides: Surprises from simple systems. *Acc. Chem. Res.* **1989,** *22* (8), 268-275.

45. Bagno, A.; Scorrano, G., Selectivity in Proton Transfer, Hydrogen Bonding, and Solvation. *Acc. Chem. Res.* **2000,** *33* (9), 609-616.

46. Zahn, D.; Schmidt, K. F.; Kast, S. M.; Brickmann, J., Quantum/Classical Investigation of Amide Protonation in Aqueous Solution. *J. Phys. Chem. A.* **2002,** *106* (34), 7807-7812.

47. Bagno, A.; Lovato, G.; Scorrano, G., Thermodynamics of protonation and hydration of aliphatic amides. *J. Chem. Soc., Perkin Trans. 2* **1993,** (6), 1091-1098.

48. Ellis, R. J.; Anderson, T. L.; Antonio, M. R.; Braatz, A.; Nilsson, M., A SAXS Study of Aggregation in the Synergistic TBP–HDBP Solvent Extraction System. *J. Phys. Chem. B.* **2013,** *117* (19), 5916-5924.

49. Ellis, R. J.; Meridiano, Y.; Muller, J.; Berthon, L.; Guilbaud, P.; Zorz, N.; Antonio, M. R.; Demars, T.; Zemb, T., Complexation-Induced Supramolecular Assembly Drives Metal-Ion Extraction. *Chem. Eur. J.* **2014,** *20* (40), 12796-12807.

50. Van Zee, N. J.; Adelizzi, B.; Mabesoone, M. F. J.; Meng, X.; Aloi, A.; Zha, R. H.; Lutz, M.; Filot, I. A. W.; Palmans, A. R. A.; Meijer, E. W., Potential enthalpic energy of water in oils exploited to control supramolecular structure. *Nature* **2018,** *558* (7708), 100-103.

51. Walton, J., Microhydration and the Enhanced Acidity of Free Radicals. *Molecules* **2018,** *23* (2), 423.

52. Gutberlet, A.; Schwaab, G.; Birer, Ö.; Masia, M.; Kaczmarek, A.; Forbert, H.; Havenith, M.; Marx, D., Aggregation-Induced Dissociation of $HCl(H_2O)_4$ Below 1 K: The Smallest Droplet of Acid. *Science* **2009,** *324* (5934), 1545-1548.

53. Gaussian 09, Revision E.01, M. J. Frisch, G. W. Trucks, H. B. Schlegel, G. E. Scuseria, M. A. Robb, J. R. Cheeseman, G. Scalmani, V. Barone, B. Mennucci, G. A. Petersson, H. Nakatsuji, M. Caricato, X. Li, H. P. Hratchian, A. F. Izmaylov, J. Bloino, G. Zheng, J. L. Sonnenberg, M. Hada, M. Ehara, K. Toyota, R. Fukuda, J. Hasegawa, M. Ishida, T. Nakajima, Y. Honda, O. Kitao, H. Nakai, T. Vreven, J. A. Montgomery, Jr., J. E. Peralta, F. Ogliaro, M. Bearpark, J. J. Heyd, E. Brothers, K. N. Kudin, V. N. Staroverov, R. Kobayashi, J. Normand, K. Raghavachari, A. Rendell, J. C. Burant, S. S. Iyengar, J. Tomasi, M. Cossi, N. Rega, J. M. Millam, M. Klene, J. E. Knox, J. B. Cross, V. Bakken, C. Adamo, J. Jaramillo, R. Gomperts, R. E. Stratmann, O. Yazyev, A. J. Austin, R. Cammi, C. Pomelli, J. W. Ochterski, R. L. Martin, K. Morokuma, V. G. Zakrzewski, G. A. Voth, P. Salvador, J. J. Dannenberg, S. Dapprich, A. D. Daniels, Ö. Farkas, J. B. Foresman, J. V. Ortiz, J. Cioslowski, and D. J. Fox, Gaussian, Inc., Wallingford CT, 2013.

54. Zhao, Y; Truhlar, D. G. The M06 suite of density functionals for main group thermochemistry, thermochemical kinetics, noncovalent interactions, excited states, and transition

elements: two new functionals and systematic testing of four M06-class functionals and 12 other functionals, *Theor. Chem. Acc.*, **2018**, *120*, 215-41

55. Hay, P. J.; Wadt, W. R. Ab initio effective core potentials for molecular calculations – potentials for the transition-metal atoms Sc to Hg, *J. Chem. Phys.*, **1985**, *82*, 270-83

56. a) Jorgensen, W. L.; Maxwell, D. S.; Tirado-Rives, J. Development and Testing of the OPLS All-Atom Force Field on Conformational Energetics and Properties of Organic Liquids, *J. Am. Chem. Soc.*, **1996**, *118*, 11225-11236. b) Plimpton, S. Fast Parallel Algorithms for Short-Range Molecular Dynamics, *J. Comp. Phys.*, **1995**, *117*, 1-19

57. a) Sheldrick, G. M. Crystal structure refinement with *SHELXL*, *Acta Crystallogr. Sect. A* **2015**, *71*, 3-8; b) Sheldrick, G. M. Crystal structure refinement with *SHELXL, Acta Crystallogr. Sect. C* **2015**, *71*, 3-8; c) Sheldrick, G. M. A short history of *SHELX*, *Acta Crystallogr. Sect. A* **2008**, *64*, 112-122.

58. Dolomanov, O. V.; Bourhis, L. J.; Gildea, R. J.; Howard, J. A. K.; Puschmann, H. *OLEX2*: a complete structure solution, refinement and analysis program, *J. Appl. Cryst.* **2009**, *42*, 339-341.

Gold is separated from a mixture of metals representing electronic waste using simple amides in solvent extraction experiments as dynamic molecular structures in the non-polar phase.

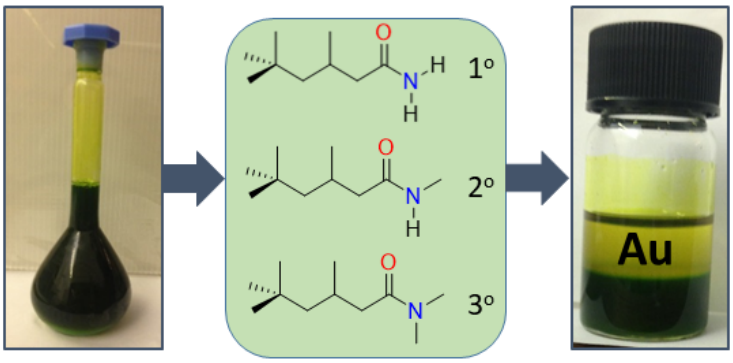

Separating Au from Electronic Waste